Estimate of breaking of ρ-A_2 exchange degeneracy in Fermilab data*

Hiroshi Nakata†
Department of Physics, University of California, Los Angeles, California 90024
(Received 30 June 1977)

Breaking of ρ-A_2 exchange degeneracy is estimated by means of simultaneous analyses of Fermilab $(d\sigma/dt)_0^{\mathrm{CEX}}$ data for $\pi^- p \to \pi^0 n$ and $\pi^- p \to \eta^0 n$ ($\eta^0 \to 2\gamma$). The result, i.e., ϵ [$\equiv \alpha_{A2}/\alpha_\rho = (\beta_{Kp}^{A2}/\beta_{Kp}^{\rho})^{1/2}$] $= 0.820 \pm 0.005$, which is obtained from these analyses is used to make further estimate of $(d\sigma/dt)_0^{\mathrm{CEX}}$ for $K^- p \to \bar{K}^0 n$ and $K^+ n \to K^0 p$ at $p_{\mathrm{lab}} = 10$ to 1000 GeV/c. In the test of kaon-nucleon total-cross-section differences, the agreement between theory and experiment for various kinds of quantities is found to be excellent, especially at $p_{\mathrm{lab}} = 100$ GeV/c. This suggests that the recent Fermilab data for the kaon-nucleon total cross sections can be successfully interpreted with the normal Regge-pole theory.

I. INTRODUCTION

Although the ρ-A_2 exchange degeneracy (EXD) relation can be well studied in the following pseudoscalar meson vs baryon charge-exchange (CEX) reactions, each of which is dominated by both ρ exchange and A_2 exchange,[1-5]

$$K^- p \to \bar{K}^0 n\,, \tag{1}$$

$$K^+ n \to K^0 p\,, \tag{2}$$

there are not so many useful data at high energies.

On the other hand, the recent Fermilab data for the companion CEX processes[6,7]

$$\pi^- p \to \pi^0 n\,, \tag{3}$$

$$\pi^- p \to \eta^0 n \tag{4}$$

enable us to examine the ρ-A_2 EXD relation indirectly, because the former process and the latter process are dominated by ρ exchange and A_2 exchange, respectively.

The Fermilab data show that the ρ and A_2 seem not to be exchange degenerate at small t. They are described in the following way:

$$\alpha_\rho(0) = 0.481 \pm 0.004, \quad \beta_\rho = 2340 \pm 80\ \mu\mathrm{b/GeV}^2 \tag{5}$$

for $\pi^- p \to \pi^0 n$ at 20–200 GeV/c,[6]

$$\alpha_{A_2}(0) = 0.371 \pm 0.008,$$

$$\beta_{A_2} = 306 \pm 27\ \mu\mathrm{b/GeV}^2 \tag{6}$$

for $\pi^- p \to \eta^0 n$ at 20–200 GeV/c,[7]

$$\text{where } (d\sigma/dt)_0^{\mathrm{CEX}} = \beta p^{2\alpha-2} \tag{7}$$

and p is in GeV/c. This indicates that there should be some breaking of EXD, because Eqs. (5) and (6) are very different. This broken EXD is experimentally confirmed by others; it is said that the differential cross section for the "real" reaction, e.g., Eq. (2) is larger than the corresponding "rotating" reaction, e.g., Eq. (1) at least at energies below 6 GeV.

Motivated by these deviations and because of the suspicious α_ρ value of Eq. (5), we reexamine the ρ-A_2 EXD problem by analyzing the Fermilab data for Eqs. (3) and (4) to make a reasonable elucidation.

II. REGGE-TRAJECTORY FUNCTION AND RESIDUE FUNCTION FOR THE ρ MESON

Parameters α_ρ and $\beta_{\pi p}^{\rho}$ are evaluated in many references. Carroll *et al.*[8] obtained $\alpha_\rho = 0.55 \pm 0.03$ from 10 data fitted between 10 and 240 GeV/c to

$$\Delta\sigma_t(\pi^\pm p) = \sigma_t(\pi^- p) - \sigma_t(\pi^+ p) = A s^{\alpha-1}\,.$$

The empirical fit[9] to 17 data between 8 and 240 GeV/c is represented by $\Delta\sigma(\pi^\pm p) = 5606\, p^{-0.455}$ and $\alpha_\rho = 0.545$, where $\Delta\sigma$ and p are in μb and GeV/c, respectively.

Hendrick *et al.*[10] obtained $\Delta\sigma(\pi^\pm p) = 5.24 \times 10^3 p^{-0.43}$ and $\alpha_\rho = 0.57 \pm 0.01$ from old data between 5 and 200 GeV/c. Barnes *et al.*[6] obtained Eq. (5) for $(d\sigma/dt)_0^{\pi^- p \to \pi^0 n}$ between 20 and 200 GeV/c.

These α_ρ values are accurate enough to reproduce data in their respective fits, but the α_ρ value obtained from Eq. (5) is not in good agreement with the other α_ρ values obtained from $\Delta\sigma(\pi^\pm p)$, as stated above.

According to the $\rho + \rho'$ Regge-pole analysis between 8 and 240 GeV/c with the dual resonance model,[11] it is found that Regge parameters

$$\alpha_1 = 0.470 \pm 0.005, \quad \beta_1 = 142.71\ \mu\mathrm{b}^{1/2}, \tag{8}$$

$$\alpha_2 = -1.80 \pm 0.1, \quad \beta_2 = -17990\ \mu\mathrm{b}^{1/2}, \tag{9}$$

which appear in the equations

$$\Delta\sigma(\pi^\pm p) = \frac{1}{p}(\beta_1 s^{\alpha_1} + \beta_2 s^{\alpha_2}) \simeq \beta_1 s^{\alpha_1} p^{-1}\,, \tag{10}$$

$$\left(\frac{d\sigma}{dt}\right)_0^{\pi^- p\to\pi^0 n} = \frac{1}{8\pi p^2}|A_0'|^2 = \frac{1}{8\pi p^2}|A_1'+A_2'|^2, \tag{11}$$

$$r = \mathrm{Re}A_0'/\mathrm{Im}A_0', \tag{12}$$

can approximately reproduce the respective experimental data. In spite of the large value of $|\beta_2|$, the ρ' component decreases rapidly with increasing energy, to play a role in the secondary correction term in comparison with the ρ component. Here suffixes 1 and 2 denote ρ and ρ', respectively.

Let us employ this α_ρ value in the following calculation, and rewrite everything in the same units and symbols as those of Hendrick *et al.*[10] They describe

$$\sigma_{ab}(s) = \frac{1}{p_{1ab}}\,\mathrm{Im}\,T_{ab\to ab}(s,0) \tag{13}$$

for the total cross section,

$$(d\sigma/dt) = \frac{1}{16\pi}\frac{|T|^2}{p_{1ab}^2} \tag{14}$$

for the differential cross section, and

$$\beta_{ab}^i(t)\left(\frac{\mp 1 - e^{-i\pi\alpha_i}}{\sin\pi\alpha_i}\right)p_{1ab}^{\alpha_i} \tag{15}$$

for the contribution of a normal Regge pole with trajectory $\alpha_i(t)$ to $T_{ab\to ab}$, where

$$\beta_{ab}^i = \gamma_a^i\gamma_b^i \tag{16}$$

and the minus sign (or plus sign) applies to even- (or odd-) signature trajectories.

Let us parametrize $\Delta\sigma(\pi^\pm p) = kp^{-n}$ for Eq. (10), to obtain $\alpha_1 = \alpha_\rho$, $\beta_{\pi p}^\rho = k/2$, and $n = 1-\alpha_\rho$, as shown in Table I, where three cases (I, II, and III) are chosen. Note that α_2 is set to -1.80 in every case.

III. ESTIMATE OF BREAKING OF ρ-A_2 EXCHANGE DEGENERACY

Since the α_{A_2} value in Eq. (6) which is obtained from $\pi^- p\to\eta^0 n$ is clearly smaller than the value in Eq. (8) which is obtained from $\pi^- p\to\pi^0 n$, the normal EXD relation cannot be accepted in any sense. The α_ρ value which is restricted by Eq. (8) is absolutely larger than the α_{A_2} value. In this section, we explore the breaking of ρ-A_2 EXD (in the spirit of strong EXD) at 20–200 GeV/c on the basis of the α_{A_2} in Eq. (6) and the α_ρ in Eq. (8) instead of the α_ρ which is given by Eq. (5).

Assume some breaking as follows in the sense of strong EXD:

$$\gamma_{pn}^{A_2} = \sqrt{2}\,\gamma_p^{A_2} = \sqrt{2}\,\epsilon\gamma_p^\rho, \tag{17}$$

$$\gamma_{\pi\eta}^{A_2} = \frac{2}{\sqrt{3}}\gamma_K^{A_2} = \frac{2}{\sqrt{3}}\epsilon\gamma_K^\rho, \tag{18}$$

$$\alpha_{A_2} = \epsilon\alpha_\rho, \tag{19}$$

where the π^--η-A_2 coupling is predicted by the SU(3) relation.

If another SU(3) relation or ρ universality

$$\gamma_K^\rho = \tfrac{1}{2}\gamma_\pi^\rho, \tag{20}$$

i.e.,

$$\beta_{Kp}^\rho = \tfrac{1}{2}\beta_{\pi p}^\rho \tag{21}$$

is assumed, the differential cross-section formula

TABLE I. Parameters calculated from the $\rho+\rho'$ Regge-pole analysis and some theoretical values for $\Delta\sigma(\pi^\pm p) = \sigma(\pi^- p) - \sigma(\pi^+ p)$ in mb and $(d\sigma/dt)_0^{\pi^- p\to\pi^0 n}$ in μb/(GeV/c)^2, compared with experimental data. Note that the π beam momentum p in the experiment has some experimental error. These results show that α_1, i.e., α_ρ in Eq. (19) should be 0.470 ± 0.005, while α_2 may be located between -1.7 and -1.9.

	Case I		Case II		Case III			
	$\alpha_1 = 0.46639$ $\alpha_2 = -1.80$ $\beta_1 = 5.722$ mb $k = 7.674$ mb (α_1 = lower limit for α_ρ)		$\alpha_1 = 0.470$ $\alpha_2 = -1.80$ $\beta_1 = 5.632$ mb $k = 7.571$ mb		$\alpha_1 = 0.475$ $\alpha_2 = -1.80$ $\beta_1 = 5.509$ mb $k = 7.429$ mb (α_1 = upper limit for α_ρ)		Experimental data	
							Ref. 8	Ref. 6
P_{lab} (GeV/c)	$\Delta\sigma$	$\left(\frac{d\sigma}{dt}\right)_0$	$\Delta\sigma$	$\left(\frac{d\sigma}{dt}\right)_0$	$\Delta\sigma$	$\left(\frac{d\sigma}{dt}\right)_0$	$\Delta\sigma$	$\left(\frac{d\sigma}{dt}\right)_0$
20	1.517	108.5	1.514	109.2	1.511	110.3	···	100.3 ± 5
50	0.952	41.98	0.952	42.47	0.953	43.16	0.94 ± 0.06	···
100	0.658	20.04	0.660	20.37	0.663	20.84	0.67 ± 0.06	19.51 ± 0.8
150	0.530	12.99	0.533	13.24	0.536	13.61	0.61 ± 0.04	12.88 ± 0.5
200	0.455	9.55	0.457	9.76	0.460	10.05	0.48 ± 0.06	9.61 ± 0.4

TABLE II. Theoretical $(d\sigma/dt)_0$ values in μb/ (GeV/c)^2 for $\pi^- p \to \eta^0 n$ ($\eta^0 \to 2\gamma$) with the ρ-A_2 EXD parameter ϵ, compared with experimental data as a function of p, where Eq. (20) or Eq. (21) is assumed. Parameters α_1, α_2, β_1, and k for cases I, II, and III are shown in Table I. The agreement is quite good. Note that the α_ρ value must be located between case I and case III. Hence the ϵ value should be 0.81 and 0.83 at worst. Finer calculation assures us that it is between 0.820 and 0.825.

		Eq. (22) for case I			Eq. (22) for case II			Eq. (22) for case III		
P_{lab} (GeV/c)	Experimental data (Ref. 7)	ϵ 0.81	ϵ 0.82	ϵ 0.83	ϵ 0.81	ϵ 0.82	ϵ 0.83	ϵ 0.81	ϵ 0.82	ϵ 0.83
20.8	6.71 ± 1.0	6.01	6.35	6.71	5.87	6.21	6.57	5.69	6.02	6.37
40.8	2.88 ± 0.36	2.60	2.76	2.94	2.55	2.71	2.89	2.48	2.64	2.81
64.4	1.62 ± 0.20	1.47	1.57	1.68	1.45	1.55	1.65	1.42	1.51	1.62
100.7	0.92 ± 0.12	0.844	0.906	0.971	0.832	0.893	0.959	0.817	0.877	0.942
150.2	0.558 ± 0.08	0.513	0.553	0.595	0.507	0.546	0.589	0.499	0.538	0.580
199.3	0.391 ± 0.06	0.361	0.390	0.421	0.357	0.386	0.417	0.353	0.381	0.412
500.0	· · ·	0.115	0.125	0.136	0.114	0.125	0.136	0.114	0.124	0.135
1000.0	· · ·	0.0485	0.0532	0.0582	0.0485	0.0532	0.0583	0.0484	0.0532	0.0584

for $\pi^- p \to \eta^0 n$ ($\eta^0 \to 2\gamma$) at $t = 0$ is represented by Eq. (14) as follows:

$$\left(\frac{d\sigma}{dt}\right)_0^{\eta \to 2\gamma} = \frac{\xi}{6\pi} \frac{\epsilon^4 (\beta_{Kp}^{\rho})^2}{\sin^2(\frac{1}{2}\pi\epsilon\alpha_\rho)} p^{2\epsilon\alpha_\rho - 2} \tag{22}$$

where $\xi = \Gamma_{\eta \to 2\gamma}/\Gamma_{total} = 0.38 \pm 0.01$ (according to Ref. 12). It is evident that Eq. (16) allows the Regge residue to be described as

$$\beta_{Kp}^{A_2} = \epsilon^2 \beta_{Kp}^{\rho} \tag{23}$$

in this assumption.

Table II shows some of the results of the calculations for $\epsilon = 0.81 - 0.83$ at 20–200 GeV/c in comparison with Fermilab data.[7] The results are seen to depend upon α_ρ, ϵ, and p. The agreement is excellent.

Table III shows some results of the calculation for $\epsilon = 1$. These results tell us that $\epsilon = 1$ cannot be accepted, but ϵ should be located between 0.81 and 0.83 in the case of $\alpha_\rho = 0.470 \pm 0.005$. Thus the quantity of $\epsilon [\equiv \alpha_{A_2}/\alpha_\rho = (\beta_{Kp}^{A_2}/\beta_{Kp}^{\rho})^{1/2}]$ which is considered to correspond to the degree of breaking of ρ-A_2 EXD is

$$\epsilon = 0.82 \pm 0.005 \tag{24}$$

in the spirit of strong EXD. In other words, Eqs. (8), (9), (19), (23), and (24) are so consistent that Eqs. (10), (11), (12), and (22) can agree with their respective experimental data to a considerable extent at the same time.

In this analysis for $\pi^- p \to \eta^0 n$ ($\eta^0 \to 2\gamma$), Eq. (22) depends more strongly on α_ρ than ϵ. It is therefore necessary to determine the α_ρ value precisely before discussing the accurate value for ϵ. In the case of Eq. (5), it is impossible to find good agreement between theory and experiment for Eq. (22) whatever ϵ may be. Therefore Eq. (5) is not used in this study.

This broken exchange degeneracy asserts that α_ρ (= 0.470 ± 0.005) is larger than α_{A_2} (= 0.385 ± 0.005).[13]

IV. ESTIMATE OF $(d\sigma/dt)_0$ FOR $K^- p \to \bar{K}^0 n$ AND $K^+ n \to K^0 p$

This breaking of ρ-A_2 EXD provides us with the estimate of $(d\sigma/dt)_0$ for $K^- p \to \bar{K}^0 n$ and $K^+ n \to K^0 p$, i.e.,

$$\left(\frac{d\sigma}{dt}\right)_0^{K^- p \to \bar{K}^0 n} = \lambda + \mu - \nu, \tag{25}$$

$$\left(\frac{d\sigma}{dt}\right)_0^{K^+ n \to K^0 p} = \lambda + \mu + \nu, \tag{26}$$

which are derived from

$$T_{K^- p \to \bar{K}^0 n} = -2(T_{Kp}^{\rho} + T_{Kp}^{A_2}), \tag{27}$$

$$T_{K^+ n \to K^0 p} = -2(T_{Kp}^{\rho} - T_{Kp}^{A_2}), \tag{28}$$

with Eqs. (19) and (23), respectively, where

TABLE III. Theoretical $(d\sigma/dt)_0$ values in μb/(GeV/c)^2 for $\pi^- p \to \eta^0 n$ ($\eta^0 \to 2\gamma$) with $\epsilon = 1$, where Eq. (20) or Eq. (21) is assumed. Parameters for case I, II, and III are shown in Table I. Note that the value of Eq. (22) in the case of $\epsilon = 1$ never agrees with the experimental value which is shown in Table II. This is due to the fact that the ϵ value is not equal to 1.

P_{lab} (GeV/c)	Eq. (22) for case I	Eq. (22) for case II	Eq. (22) for case III
20.8	16.71	16.41	16.01
40.8	8.14	8.03	7.89
64.4	5.00	4.95	4.89
100.7	3.10	3.08	3.06
150.2	2.03	2.02	2.01
199.3	1.50	1.50	1.49

TABLE IV. Theoretical $(d\sigma/dt)_0$ values in μb/(GeV/c)^2 for $K^-p \to \bar{K}^0 n$ and $K^+n \to K^0 p$ with $\epsilon = 0.81$, 0.82, or 0.83, where only case II is considered. This prediction is very close to available data[14] at lower momenta, below 40 GeV/c.

ϵ	$P_{\rm lab}$ (GeV/c)	Eq. (26) $K^+n \to K^0p$	Eq. (25) $K^-p \to \bar{K}^0n$	Eq. (32) Eq. (26)−Eq. (25)
0.81	10	197	151	45.7
	20	90.6	69.9	20.6
	50	32.6	25.4	7.20
	100	15.1	11.8	3.24
	150	9.63	7.59	2.04
	200	7.01	5.54	1.46
	1000	1.19	0.961	0.230
0.82	10	199	155	44.4
	20	91.7	71.6	20.1
	50	33.0	26.0	7.04
	100	15.3	12.1	3.19
	150	9.77	7.77	2.00
	200	7.11	5.67	1.44
	1000	1.21	0.980	0.228
0.83	10	201	158	43.0
	20	92.9	73.3	19.5
	50	33.5	26.6	6.87
	100	15.5	12.4	3.12
	150	9.92	7.95	1.96
	200	7.22	5.80	1.41
	1000	1.23	1.00	0.226

$$\lambda = \frac{1}{4\pi} \frac{(\beta^{\rho}_{Kp})^2}{\cos^2(\frac{1}{2}\pi\alpha_\rho)} p^{2\alpha_\rho - 2}, \tag{29}$$

$$\mu = \frac{1}{4\pi} \frac{\epsilon^4(\beta^{\rho}_{Kp})^2}{\sin^2(\frac{1}{2}\pi\epsilon\alpha_\rho)} p^{2\epsilon\alpha_\rho - 2}, \tag{30}$$

$$\nu = \frac{1}{2\pi}\epsilon^2(\beta^{\rho}_{Kp})^2\left(\tan\frac{\pi}{2}\alpha_\rho \cot\frac{\pi}{2}\epsilon\alpha_\rho - 1\right) p^{(1+\epsilon)\alpha_\rho - 2}. \tag{31}$$

Table IV shows some of the results of the calculation for $\epsilon = 0.81 - 0.83$ at 20–1000 GeV/c in the case of $\alpha_\rho = 0.470$ and $\beta_1 = 5.632$ mb. The quantity defined by

$$D = \text{Eq. (26)} - \text{Eq. (25)} \tag{32}$$

is always positive.

Table V shows some results of the calculation for $\epsilon = 0.82$. Table VI shows some results of the calculation for $\epsilon = 1$, which means no breaking of $\rho - A_2$ EXD; in this case Eqs. (25) and (26) become the same expression,

$$\left(\frac{d\sigma}{dt}\right)^{KN}_0 = \frac{1}{\pi}\left(\frac{\beta^{\rho}_{Kp}}{\sin\pi\alpha_\rho}\right)^2 p^{2\alpha_\rho - 2}, \tag{33}$$

as a matter of course.

It is obvious that the $(d\sigma/dt)_0$ value for these processes depends on ϵ in a monotonic way, but the α dependence is not monotonic. The asymptotic behavior in the case of large p is not definite because the three quantities λ, μ, and ν are not so different but satisfy

$$\lambda > \mu > \nu. \tag{34}$$

TABLE V. Theoretical $(d\sigma/dt)_0$ values in μb/(GeV/c)^2 for $K^-p \to \bar{K}^0n$ and $K^+n \to K^0p$ with $\epsilon = 0.82$, where case I and case III are shown as a function of p. See Table IV for case II.

Case	$P_{\rm lab}$ (GeV/c)	Eq. (26) $K^+n \to K^0p$	Eq. (25) $K^-p \to \bar{K}^0n$	Eq. (32) Eq. (26)−Eq. (25)
I	10	201	156	44.7
	20	92.0	71.9	20.1
	50	32.9	25.9	7.01
	100	15.2	12.0	3.16
	150	9.65	7.67	1.98
	200	7.01	5.59	1.42
	1000	1.18	0.954	0.223
III	10	197	153	44.1
	20	91.2	71.2	20.1
	50	33.2	26.1	7.09
	100	15.5	12.3	3.23
	150	9.93	7.89	2.04
	200	7.25	5.78	1.47
	1000	1.25	1.03	0.236

TABLE VI. Theoretical $(d\sigma/dt)_0$ values in μb/(GeV/c)^2 for $K^-p \to \bar{K}^0 n$ and $K^+n \to K^0 p$ with $\epsilon = 1$. In this case, Eq. (32) is exactly zero.

P_{lab} (GeV/c)	Eq. (33) for case I	Eq. (33) for case II	Eq. (33) for case III
10	261	257	253
20	124	123	122
50	46.8	46.7	46.7
100	22.3	22.4	22.5
150	14.5	14.6	14.7
200	10.7	10.8	10.9
1000	1.91	1.95	2.01

These estimates may be acceptable when p is larger than 20 GeV/c; it is approximately in agreement with the low-energy experimental data,[14] which are shown in the figure of Ref. 10.

When p goes to infinity, the D value given by Eq. (32) tends to zero, but it does not arrive at zero. This is an interesting subject for future experiment. Next the K-N total-cross-section differences are examined with these parameters since the present α_ρ and $\beta^\rho_{\pi p}$ values given by Eq. (8) have shown good results, as listed in Table II, through the simple procedure which comprises Eqs. (17) through (24).

V. KAON-NUCLEON TOTAL-CROSS-SECTION DIFFERENCES

It is very tempting to consider how deeply the recent Fermilab data on hadron-hadron interactions are connected with each other and whether they can be elucidated completely in terms of normal Regge phenomenology. A part of the relation is delineated in Fig. 1. Let us study the diagram briefly.

In the first place, the intercept of the ρ Regge pole $\alpha_\rho(0)$ and the Regge residue $\beta^\rho_{\pi p}$ have been successfully derived from the $\rho + \rho'$ Regge-pole analysis[9,11] of Fermilab data on $(d\sigma/dt)_0^{\pi^- p \to \pi^0 n}$ (Ref. 6) and $\sigma(\pi^- p) - \sigma(\pi^+ p)$ (Ref. 8). They are shown by Eq. (8), which critically dominates the subsequent calculation.

In the second place, the $\alpha_{A_2}(0)$ value and the $\beta^{A_2}_{Kp}$ value have been obtained from the A_2 Regge-pole analysis of Fermilab data on $(d\sigma/dt)_0^{\pi^- p \to \eta^0 n}$ (Ref. 7). If the relation of ρ universality [Eq. (21)] is assumed there should be a breaking of

$$\epsilon \left[\equiv \alpha_{A_2}/\alpha_\rho = (\beta^{A_2}_{Kp}/\beta^\rho_{Kp})^{1/2} \right] = 0.820 \pm 0.005$$

in the sense of strong EXD, as indicated by Eqs.

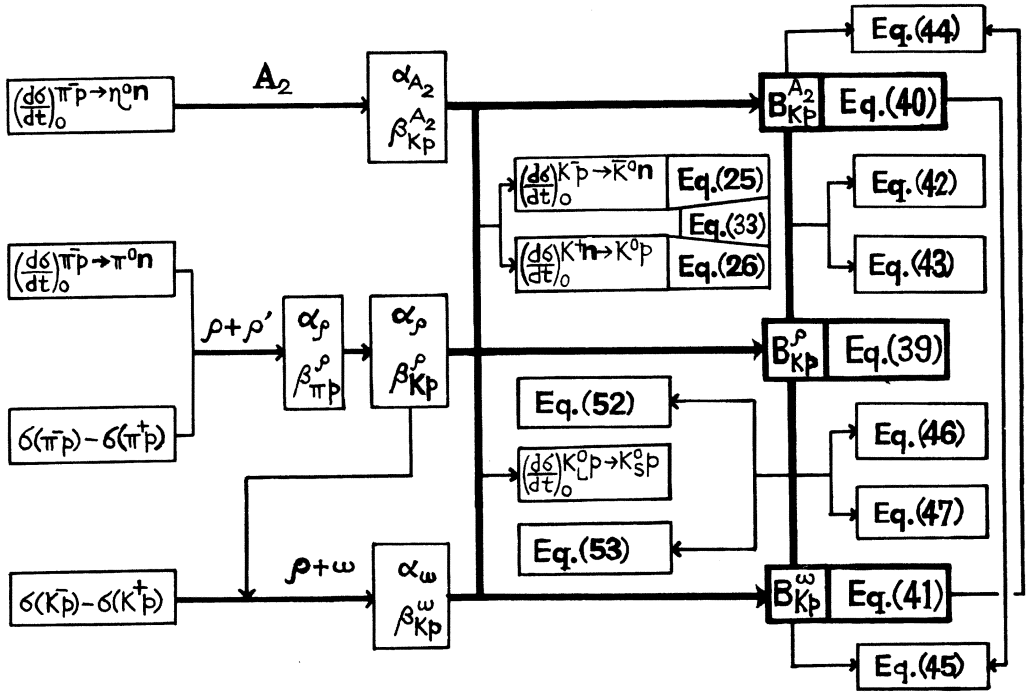

FIG. 1. Schematic diagram for the study of high-energy hadron processes which are mutually combined by Regge parameters. The symbols and equations are explained in the text.

(19) and (23). Actually it should be between 0.820 and 0.825.

In the third place, the α_ω value is evaluated from the $\rho+\omega$ Regge-pole analysis[15] of Fermilab data on $\sigma(K^-p)-\sigma(K^+p)$ (Ref. 8) with the aid of the α_ρ value and the β^ρ_{Kp} value which result from the above-mentioned $\rho+\rho'$ Regge-pole analysis.[11] Then it has turned out that the SU(3) relation between the α_ρ and the α_ω is completely satisfied.

In these analyses, it has been confirmed that available data[14] for $(d\sigma/dt)_0^{K^-p\to\bar{K}^0n}$ and $(d\sigma/dt)_0^{K^+n\to K^0p}$ at 1–35 GeV/c are in agreement with the prediction which is obtained from these parameters. No comparison between theory and experiment is possible above 50 GeV/c at present because of a lack of data. Similarly it has also been recognized that the comparison of $(d\sigma/dt)_0^{K^0_Lp\to K^0_Sp}$ between theory[15] and experiment[16] supports the conclusion that the α_ρ value is equal to the α_ω value in this regeneration process, though there are no useful data for it above 50 GeV/c.

It follows that the six parameters (α and β for ρ, ω, and A_2) which have been determined in these analyses are consistent with these seven kinds of data under the one assumption of Eq. (21). In the following subsections, it will be seen that this phenomenology is reliable and helps to make a prediction at arbitrary energies where there are no available data below 240 GeV/c.

A. Phenomenological relations for K-N total cross sections

With the notation of Hendrick *et al.*,[10] the total cross sections can be represented succinctly as follows:

$$\sigma(K^-p)=D_{Kp}+B^f_{Kp}+B^\rho_{Kp}+B^\omega_{Kp}+B^{A_2}_{Kp}, \tag{35}$$

$$\sigma(K^-n)=D_{Kp}+B^f_{Kp}-B^\rho_{Kp}+B^\omega_{Kp}-B^{A_2}_{Kp}, \tag{36}$$

$$\sigma(K^+p)=D_{Kp}+B^f_{Kp}-B^\rho_{Kp}-B^\omega_{Kp}+B^{A_2}_{Kp}, \tag{37}$$

$$\sigma(K^+n)=D_{Kp}+B^f_{Kp}+B^\rho_{Kp}-B^\omega_{Kp}-B^{A_2}_{Kp}, \tag{38}$$

where $B^i_{ab}=\beta^i_{ab}p^{\alpha_i-1}$ and D_{Kp} is the diffractive component of the Kp total cross section. Hereafter we write B^i instead of B^i_{ab}. Therefore we have

$$B^\rho=\tfrac{1}{4}[\sigma(K^-p)-\sigma(K^-n)-\sigma(K^+p)+\sigma(K^+n)], \tag{39}$$

$$B^{A_2}=\tfrac{1}{4}[\sigma(K^-p)-\sigma(K^-n)+\sigma(K^+p)-\sigma(K^+n)], \tag{40}$$

$$B^\omega=\tfrac{1}{4}[\sigma(K^-p)+\sigma(K^-n)-\sigma(K^+p)-\sigma(K^+n)], \tag{41}$$

where the left-hand side of each equation is the $\beta^i_{ab}p^{\alpha_i-1}$ quantity which is phenomenologically determined from the Regge-pole analysis of the related data, while the right-hand side of each equation is the quantity which is directly measured in the experiment.

Then kaon-nucleon total-cross-section differences can be represented by B^ρ, B^{A_2}, and B^ω as follows:

$$\sigma(K^-p)-\sigma(K^-n)=2(B^\rho+B^{A_2}), \tag{42}$$

$$\sigma(K^+p)-\sigma(K^+n)=2(-B^\rho+B^{A_2}), \tag{43}$$

$$\sigma(K^-p)-\sigma(K^+n)=2(B^{A_2}+B^\omega), \tag{44}$$

$$\sigma(K^+p)-\sigma(K^-n)=2(B^{A_2}-B^\omega), \tag{45}$$

$$\sigma(K^-p)-\sigma(K^+p)=2(B^\omega+B^\rho), \tag{46}$$

$$\sigma(K^-n)-\sigma(K^+n)=2(B^\omega-B^\rho), \tag{47}$$

where Eq. (43) is useful to test the ρ-A_2 EXD relation. Generally, neutron data are more ambiguous than proton data, because the former data are indirectly derived from the latter data subtracted from deuterium data with a certain phenomenological hypothesis concerning the Glauber correction. For this reason, Eq. (46) should be respected much more than Eq. (47) in the case of discussing numerical value.

These equations yield the following relations:

$$\sigma(K^-n)=\sigma(K^-p)-2B^\rho-2B^{A_2}, \tag{48}$$

$$\sigma(K^-n)=\sigma(K^+p)-2B^{A_2}+2B^\omega, \tag{49}$$

$$\sigma(K^+n)=\sigma(K^+p)+2B^\rho-2B^{A_2}, \tag{50}$$

$$\sigma(K^+n)=\sigma(K^-p)-2B^{A_2}-2B^\omega. \tag{51}$$

It is of significance to make a comparison between Eq. (48) and Eq. (49) for $\sigma(K^-n)$, and between Eq. (50) and Eq. (51) for $\sigma(K^+n)$. These relations show that neutron data can be checked by means of proton data and Regge theory where the Glauber correction term is not employed.

TABLE VII. Examples for numerical values of Eq. (39) and Eq. (41). Note that the prediction should be between case I and case III because the parameters must be between case I and case III.

	Eq. (39)				Eq. (41)			
P	Right-hand side	Left-hand side (mb)			Right-hand side	Left-hand side (mb)		
(GeV/c)	(mb)	Case I	Case II	Case III	(mb)	Case I	Case II	Case III
35	0.293	0.288	0.288	0.287	1.07	1.08	1.07	1.07
100	0.163	0.164	0.165	0.166	0.623	0.614	0.614	0.615
1000	···	0.048	0.049	0.049	···	0.180	0.181	0.184

TABLE VIII. Examples for numerical values of Eq. (40). Note that the prediction should be between case I and case III; besides, it is restricted by the ϵ values of 0.820 and 0.825 in each case. Therefore the ambiguity of the prediction is approximately 1 to 2%.

P (Gev/c)	Right-hand side (mb)	Left-hand side (mb) Case I $\epsilon=0.820$	Case I $\epsilon=0.825$	Case II $\epsilon=0.820$	Case II $\epsilon=0.825$	Case III $\epsilon=0.820$	Case III $\epsilon=0.825$
100	0.083	0.075	0.077	0.075	0.077	0.075	0.077
150	0.053	0.058	0.060	0.059	0.060	0.059	0.060
1000	...	0.018	0.019	0.018	0.019	0.018	0.019

TABLE IX. Examples for numerical values of Eqs. (42) and (43), where $\alpha_\rho=\alpha_\omega=0.470\pm0.005$.

P (GeV/c)	Eq. (42) (mb) Left-hand side	Right-hand side (±0.002) $\epsilon=0.820$	Right-hand side (±0.002) $\epsilon=0.825$	Eq. (43) (mb) Left-hand side	Right-hand side (±0.001) $\epsilon=0.820$	Right-hand side (±0.001) $\epsilon=0.825$
100	0.49	0.480	0.483	−0.16	−0.180	−0.176
170	0.40	0.357	0.360	−0.10	−0.140	−0.138
1000	...	0.134	0.135	...	−0.061	−0.060

TABLE X. Examples for numerical values of Eqs. (44) and (45), where $\alpha_\rho=\alpha_\omega=0.470\pm0.005$ and $\epsilon=0.820$.

P (GeV/c)	Eq. (44) (mb) Left-hand side	Right-hand side (±0.01)	Eq. (45) (mb) Left-hand side	Right-hand side (±0.01)
35	2.25	2.43	−2.02	−1.86
100	1.41	1.38	−1.08	−1.08
1000	...	0.40	...	−0.33

TABLE XI. Examples for numerical values of Eqs. (46) and (47), where $\alpha_\rho=\alpha_\omega=0.470\pm0.005$.

P (GeV/c)	Eq. (46) (mb) Left-hand side	Right-hand side (±0.01)	Eq. (47) (mb) Left-hand side	Right-hand side (±0.01)
35	2.72	2.72	1.55	1.57
100	1.57	1.56	0.92	0.90
1000	...	0.46	...	0.27

TABLE XII. Examples for numerical values of Eqs. (48), (49), (50), and (51), where $\alpha_\rho=\alpha_\omega=0.470$ and $\epsilon=0.820$.

P (GeV/c)	Left-hand side (mb)	Right-hand side (mb) Eq. (48)	Right-hand side (mb) Eq. (49)	Left-hand side (mb)	Right-hand side (mb) Eq. (50)	Right-hand side (mb) Eq. (51)
35	19.84	19.68	19.68	18.29	18.11	18.11
100	19.96	19.97	19.96	19.04	19.06	19.07
170	20.25	20.29	20.46	19.74	19.78	19.61

B. Results of calculations

For a rigorous comparison between theory and experiment, some results of the calculations are given in Tables VII–XII.

Table VII shows the individual comparison between the right-hand side and the left-hand side for Eq. (39) and Eq. (41), where cases I, II, and III correspond to $\alpha_\rho = \alpha_\omega = 0.46639$, 0.470, and 0.475, respectively.[11,15]

Table VIII shows the comparison of the right-hand side with the left-hand side of Eq. (40), where $\epsilon = 0.820$ or 0.825. By reviewing these results, it will be found that Eqs. (39) and (41) are approximately satisfied. However, no conclusion about Eq. (40) can be extracted from Table VIII since the fluctuation of the experimental data is fairly large.

Table IX shows the comparison between the right-hand side and the left-hand side for Eq. (42) and Eq. (43). The left-hand side of Eq. (43) which is the experimental value for the ρ-A_2 EXD relation is by no means zero. Then it assures us that the ρ-A_2 EXD relation is absolutely broken. The right-hand side of Eq. (43) which is phenomenologically calculated by the parameters for A_2, which have been determined from the analysis of $(d\sigma/dt)_0^{\pi^- p \to \eta^0 n}$ data,[7] never vanishes. Therefore in terms of the EXD, the two sets of Fermilab data $\sigma(K^+p) - \sigma(K^+n)$ (Ref. 8) and $(d\sigma/dt)_0^{\pi^- p \to \eta^0 n}$ (Ref. 7) are entirely consistent. Apparently the data[8] at $p = 50$ and 200 GeV/c seem wrong.

Table X shows the comparison between the right-hand side and the left-hand side for Eqs. (44) and (45). While Eq. (44) is acceptable in the whole momentum range, that data above 170 GeV/c for Eq. (45) drop sharply. This phenomenon is also observed in the data for $\sigma(K^-p) - \sigma(K^+p)$ in Eq. (46) and $\sigma(K^-n) - \sigma(K^+n)$ in Eq. (47), which are given in Table XI. Incidentally, let us indicate the fact that something is strange in Table I of Ref. 8, where $\sigma(K^-n) - \sigma(K^+n)$ is 0.94 ± 0.20 mb at 200 GeV/c, which seems to be extraordinarily high.

Table XII shows the comparison between the right-hand side and the left-hand side for Eqs. (48) through Eq. (51).

VI. DISCUSSION

First of all, we should take a look at the experimental error in these data. Firgure 2 depicts the results of the calculation in comparison with data, some of which fluctuate more or less in terms of the momentum of incident kaons. For example, the right-hand side of Eq. (39) at $p = 200$ GeV/c

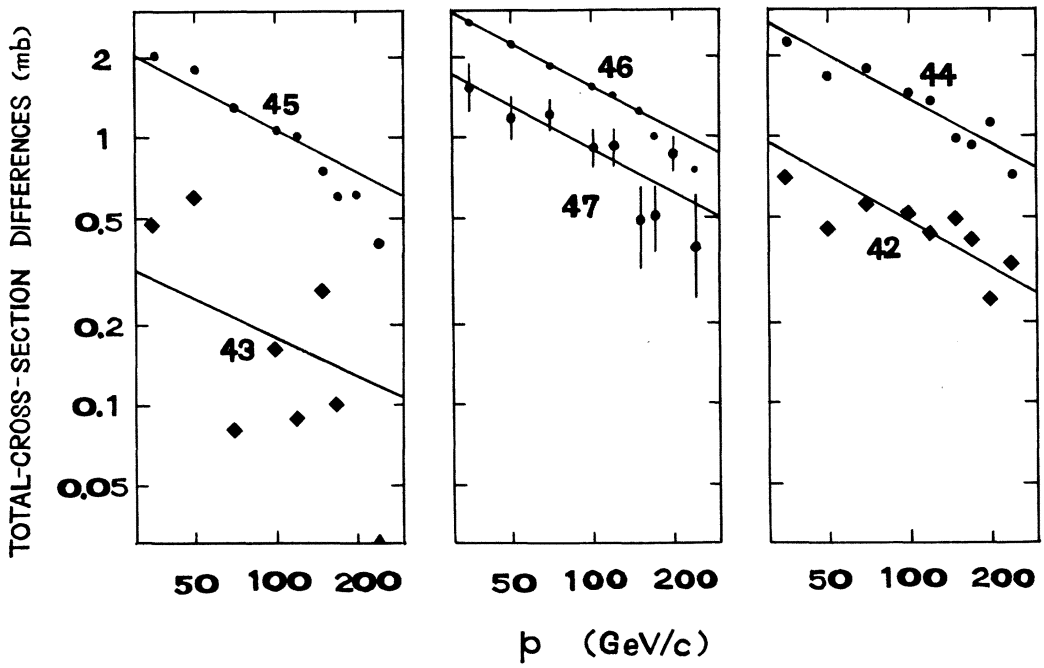

FIG. 2. Comparison of K-N total-cross-section differences between the right-hand side (theoretical prediction: solid line) and the left-hand side (Fermilab data: dot) for Eqs. (42), (43), (44), (45), (46), and (47). Note that the absolute value is shown in the case of Eqs. (43) and (45) since they are always negative. The agreement is excellent, especially at $p = 100$ GeV/c.

and that of Eq. (40) at $p=50$ GeV/c are negative, whereas those at the other momenta are all positive. We cannot quote these data at $p=50$ or 200 GeV/c for the comparison between theory and experiment since they break the phenomenological systematics. The experimental $\sigma(K^+n)$ values at $p=50$ and 200 GeV/c look strange in a strict sense.

Let us indicate another important fact: The data for $\sigma(K^-p)-\sigma(K^+p)$ in Eq. (46) suddenly drop between 170 and 240 GeV/c. As mentioned in Ref. 15, they might have an unexpected experimental error (or a sophisticated high-energy hadron behavior). For these reasons, we will consider the comparison principally from 70 to 150 GeV/c in each case.

The approximate agreement between theory and experiment in this study means that each value for the α_ρ, α_ω, α_{A_2}, β^ρ_{Kp}, β^ω_{Kp}, and $\beta^{A_2}_{Kp}$ parameters is reasonable, and these values support the two conclusions that the ρ-A_2 EXD relation is broken but the ρ-ω SU(3) relation is satisfied under the assumption of ρ universality.

The latter relation ($\alpha_\rho=\alpha_\omega$) can be reexamined by the ratio of Eq. (41) to Eq. (39),

$$\frac{B^\omega}{B^\rho}=\frac{\sigma(K^-p)+\sigma(K^-n)-\sigma(K^+p)-\sigma(K^+n)}{\sigma(K^-p)-\sigma(K^-n)-\sigma(K^+p)+\sigma(K^+n)} \quad (52)$$

and another ratio of Eq. (47) to Eq. (46),

$$\frac{B^\omega-B^\rho}{B^\omega+B^\rho}=\frac{\sigma(K^-n)-\sigma(K^+n)}{\sigma(K^-p)-\sigma(K^+p)}\,, \quad (53)$$

where the left-hand sides of Eqs. (52) and (53) are 3.73 and 0.577, respectively, and independent of p in the case of $\alpha_\rho=\alpha_\omega=0.470$. It should be noted that the denominator and numerator of the right-hand side of Eq. (52) or Eq. (53) asymptotically goes to zero, owing to the Pomeranchuk theorem. As shown in Table XIII, Eq. (52) and Eq. (53) are approximately acceptable. It follows that the model ($\alpha_\rho=\alpha_\omega$) is approximately acceptable with no serious difficulty.

Let us make a general observation again. Because of the virtual neutron target, the left-hand sides of Eq. (47) through Eq. (51) are more or less uncertain. The right-hand sides are useful to provide the prediction for $\sigma(K^-n)$ or $\sigma(K^+n)$ on the basis of $\sigma(K^+p)$ or $\sigma(K^-p)$. On the other hand, the agreement between theory and experiment for any quantity in Tables IX through XIII is excellent especially at 100 GeV/c. This seems to suggest that all four fundamental data $\sigma(K^-p)$, $\sigma(K^+p)$, $\sigma(K^-n)$, and $\sigma(K^+n)$ at 100 GeV/c are good. It may be expected that these theoretical values will agree very well with data if remeasurements are performed for the stringent test of these relations, since the cross-section difference is sometimes subject to a large experimental error and is difficult to evaluate.

TABLE XIII. Examples for numerical values of Eqs. (52) and (53) where $\alpha_\rho=\alpha_\omega=0.470$; in this case the left-hand side, i.e., the theoretical values for Eqs. (52) and (53) are 3.73 and 0.577, respectively. The agreement of the value between the left-hand side and the right-hand side of each equation supports the present model. More precise data, however, are required for its stringent testing.

P (GeV/c)	Right-hand side of Eq. (52)	Right-hand side of Eq. (53)
35	3.64	0.570
100	3.83	0.586
240	3.11	0.514

Anyway the role of the ρ intercept is crucial in the connection for various kinds of data in Fig. 1. Everything is dominated by the α_ρ value which is determined from the concepts of Regge pole and duality in the initial step of the approach to this problem. However, this is plagued with one problem. If we apply the mass and spin for the ρ and the ω (Ref. 12) to the Regge trajectory function

$$\alpha(t)=\alpha(0)+\alpha' t\,, \quad (54)$$

we cannot lead to

$$\alpha_\rho(0)=\alpha_\omega(0)\,, \quad (55)$$

in contrast to the conclusion ($\alpha_\rho=\alpha_\omega$) which is shown in Ref. 15. Equation (54) has a linear and parallel trajectory for any Regge pole. Because of $m_\rho\neq m_\omega$, Eq. (55) cannot be established in an exact sense; otherwise at least the concept of universal slope must be replaced with something else. Table XIII, Eqs. (52), and (53) support $\alpha_\rho=\alpha_\omega$.

The B terms for the ρ, ω, and A_2 in Eqs. (35)–(38) allow the common, remaining $D_{Kp}+B^f_{Kp}$ term to be easily determined by a semiempirical method.[17]

Finally we should compare the present results with those of Hendrick *et al.*[10] In the present study we have

$$\alpha_\rho=0.470\pm0.005,\quad \alpha_\omega=0.470\pm0.005\,,$$

$$\alpha_{A_2}/\alpha_\rho=0.820\pm0.005,\quad \beta^{A_2}_{Kp}/\beta^\rho_{Kp}=0.672\pm0.01\,,$$

while Hendrick *et al.* obtained $\alpha_\rho=0.57\pm0.01$, $\alpha_\omega=0.43\pm0.01$ to confirm $\alpha_\rho/\alpha_\omega=1.32\pm0.04$. They assumed that $\alpha_{A_2}/\alpha_\rho=1$ and found that theory and experiment did not agree very well in the case of $(d\sigma/dt)_0$ for $\pi^-p\to\eta^0n\to2\gamma+n$. Although their results shown in Fig. 8 of Ref. 10 are said to show the agreement between theory and experiment in the case of $(d\sigma/dt)_0$ for $K^-p\to\bar{K}^0n$ and

TABLE XIV. Summary for comparison between theory and experiment. The overall agreement is fairly good in consideration of large experimental errors.

Input data	Experiment	Results of calculation
$(d\sigma/dt)_0$ for $\pi^- p \to \pi^0 n$	Ref. 6	Refs. 9 and 11
$\sigma(\pi^- p) - \sigma(\pi^+ p)$	Ref. 8	Refs. 9 and 11
$(d\sigma/dt)_0$ for $\pi^- p \to \eta^0 n$	Ref. 7	Tables II and III
$\sigma(K^- p) - \sigma(K^+ p)$	Ref. 8	Ref. 15 (selected data)

Values of parameters	Relation	Note
$0.465 < \alpha_\rho < 0.475$ (Refs. 9 and 11)		Case I: $\alpha_\rho = 0.46639$
$0.465 < \alpha_\omega < 0.475$ (Ref. 15)	$\alpha_\rho = \alpha_\omega$	Case II: $\alpha_\rho = 0.470$
$0.380 < \alpha_{A_2} < 0.390$ (Table II)	Eq. (19)	Case III: $\alpha_\rho = 0.475$
$0.820 < \epsilon < 0.825$ (Eq. (24))	Eq. (23)	Eq. (21) is assumed

Output data	Experiment	Theory	Reference
$(d\sigma/dt)_0$ for $K^- p \to \bar{K}^0 n$	No data above 50 GeV/c	Eqs. (25) and (33)	Tables IV, V, and VI
$(d\sigma/dt)_0$ for $K^+ n \to K^0 p$	No data above 50 GeV/c	Eqs. (26) and (33)	Tables IV, V, and VI
$(d\sigma/dt)_0$ for $K_L^0 p \to K_S^0 p$	No data above 50 GeV/c	Ref. 15	Ref. 15
$\sigma(K^- p) - \sigma(K^- n) - \sigma(K^+ p) + \sigma(K^+ n)$	Ref. 8	Eq. (39)	Table VII
$\sigma(K^- p) - \sigma(K^- n) + \sigma(K^+ p) - \sigma(K^+ n)$	Ref. 8	Eq. (40)	Table VIII
$\sigma(K^- p) + \sigma(K^- n) - \sigma(K^+ p) - \sigma(K^+ n)$	Ref. 8	Eq. (41)	Table VII
$\sigma(K^- p) - \sigma(K^- n)$	Ref. 8	Eq. (42)	Table IX; Fig. 2
$\sigma(K^+ p) - \sigma(K^+ n)$	Ref. 8	Eq. (43)	Table IX; Fig. 2
$\sigma(K^- p) - \sigma(K^+ n)$	Ref. 8	Eq. (44)	Table X; Fig. 2
$\sigma(K^+ p) - \sigma(K^- n)$	Ref. 8	Eq. (45)	Table X; Fig. 2
$\sigma(K^- p) - \sigma(K^+ p)$	Ref. 8	Eq. (46)	Table XI; Fig. 2
$\sigma(K^- n) - \sigma(K^+ n)$	Ref. 8	Eq. (47)	Table XI; Fig. 2
$\sigma(K^- n)$	Ref. 8	Eqs. (48) and (49)	Table XII
$\sigma(K^+ n)$	Ref. 8	Eqs. (50) and (51)	Table XII
$\dfrac{\sigma(K^- p) + \sigma(K^- n) - \sigma(K^+ p) - \sigma(K^+ n)}{\sigma(K^- p) - \sigma(K^- n) - \sigma(K^+ p) + \sigma(K^+ n)}$	Ref. 8	Eq. (52)	Table XIII
$\dfrac{\sigma(K^- n) - \sigma(K^+ n)}{\sigma(K^- p) - \sigma(K^+ p)}$	Ref. 8	Eq. (53)	Table XIII

$K^+ n \to K^0 p$, it is very difficult to accept this statement. Table XIV shows the summary of our results. It can be said that the normal Regge theory is established in the recent Fermilab data which are mutually connected as shown in Fig. 1. This means that no special idea is required for the discussion of Regge phenomenology. In order to understand the main trend of hadron-hadron interactions, no new term (cut or non-Regge term) is required. The relation $\alpha_\rho = \alpha_\omega$ is kept completely. The α_ρ value cannot be so high as 0.48 or 0.50 which is presented in some other publications. It should be noted that, as Eq. (23) states, $\beta_{Kp}^{A_2}/\beta_{Kp}^{\rho}$ is not ϵ but ϵ^2.

VII. SUMMARY

In this study it is found that there should be some breaking of ρ-A_2 exchange degeneracy; unless Eq. (20) or Eq. (21) for the SU(3) or ρ universality relation is broken, it is $\epsilon = \alpha_{A_2}/\alpha_\rho = (\beta_{Kp}^{A_2}/\beta_{Kp}^{\rho})^{1/2} = 0.820 \pm 0.005$, which is obtained from the simultaneous analysis of data for $\pi^- p \to \pi^0 n$ and $\pi^- p \to \eta^0 n$. Judging from the fact that the comparison between theory and experiment for kaon-nucleon total-cross-section differences is excellent (especially at 100 GeV/c) in spite of large experimental errors, we know that the values of the parameters (α_ρ, α_ω, α_{A_2}, β_{Kp}^{ρ}, β_{Kp}^{ω},

and $\beta_{Kp}^{A_2}$) and the relations ($\alpha_\rho = \alpha_\omega$, $\alpha_{A_2} = \epsilon\alpha_\rho$, and $\beta_{Kp}^{A_2} = \epsilon^2 \beta_{Kp}^{\rho}$) are suitable. At the same time it can be said that the ρ universality relation [Eq. (20) or Eq. (21)] is also acceptable.[18]

In this procedure, we have begun by discarding the α_ρ value given in Eq. (5) since it should be located absolutely between 0.465 and 0.475 as far as these data are concerned. It is recognized and should be emphasized that input data in the left-hand side of Fig. 1 can be reasonably connected to the right-hand side of Fig. 1 through the concise Regge theory if the parameters and relations are completely suitable.[19] This heuristic conclusion stems from Eqs. (19) and (21) with Eq. (24) for ϵ and Eq. (8) for α and β.

ACKNOWLEDGMENTS

I have benefited from the sophisticated lecture of Professor Paul H. Frampton at UCLA. I wish to thank three kind fellows, John Fang, David Smith, and Nord Winnan for their hospitality and encouragement. This work would not have been possible without the strong support of Professor Roy P. Haddock.

---

*Work supported in part by Japan Society, Inc.

†Present address: Minamiuemachi 1-44-3, Kishiwada, Osaka, Japan 596.

[1]M. L. Perl, *High Energy Hadron Physics* (Wiley, New York, 1974).

[2]D. Horn and F. Zachariasen, *Hadron Physics at Very High Energies* (Benjamin, Reading, Mass., 1973).

[3]V. Barger *et al.*, Nucl. Phys. B32, 93 (1971).

[4]P. H. Frampton, *Dual Resonance Models* (Benjamin, Reading, Mass., 1974).

[5]B. H. Bransden and R. G. Moorehouse, *The Pion-Nucleon System* (Princeton University Press, Princeton, N. J., 1973).

[6]A. V. Barnes *et al.*, Phys. Rev. Lett. 37, 76 (1976).

[7]O. I. Dahl *et al.*, Phys. Rev. Lett. 37, 80 (1976).

[8]A. S. Carroll *et al.*, Phys. Lett. 61B, 303 (1976).

[9]H. Nakata, Phys. Rev. D 15, 927 (1977).

[10]R. E. Hendrick *et al.*, Phys. Rev. D 11, 536 (1975).

[11]H. Nakata, Phys. Rev. D 16, 1354 (1977).

[12]Particle Data Group, Rev. Mod. Phys. 48, S1 (1976).

[13]N. Barik and B. R. Desai, Phys. Rev. D 6, 3192 (1972); A. Deren and G. Smadja, Nuovo Cimento A62, 681 (1969); G. W. Brandenburg *et al.*, Phys. Rev. D 15, 617 (1977); A. Hacinliyan and M. Koca, *ibid.* 13, 1868 (1976).

[14]V. N. Bolotov *et al.*, Serpukhov Reports Nos. IHEP 73-53, 1973 (unpublished) and 73-58, 1973 (unpublished); G. W. Brandenburg *et al.*, Phys. Rev. D 15, 617 (1977); R. Diebold *et al.*, Phys. Rev. Lett. 32, 904 (1974); K. J. Foley *et al.*, Phys. Rev. D 9, 42 (1974).

[15]H. Nakata, Report No. HN-10, 1977 (unpublished).

[16]A. D. Brody *et al.*, Phys. Rev. Lett. 26, 1050 (1971); V.K. Birulev *et al.*, Phys. Lett. 38B, 452 (1972); G. W. Brandenburg *et al.*, Phys. Rev. D 9, 1939 (1974).

[17]H. Nakata, Report No. HN-15, 1977 (unpublished). All Regge parameters including those for the Pomeron and f tensor meson are combined to reproduce all hadron-hadron total cross sections between 23 and 10^5 GeV/c in one assumption of $\beta_{Kp}^{f} = \frac{1}{2}\beta_{\pi p}^{f}$.

[18]H. Nakata, Report No. HN-14, 1977 (unpublished). When the Fermilab data for $\sigma(\pi^- p) - \sigma(\pi^+ p)$ and $\sigma(K^- p) - \sigma(K^- n) - \sigma(K^+ p) + \sigma(K^+ n)$ are combined, Eq. (20) or Eq. (21) is found to hold successfully. Therefore, it is not a simple assumption.

[19]H. Nakata, Report No. HN-12, 1977 (unpublished). Indeed, the agreement between theory and experiment is not so excellent in some cases. For example, there is some disagreeemnt in Fig. 2. This is due to the fact that some of the Fermilab data have strange aspects in terms of systematics. The features of the Fermilab data are discussed in this report.

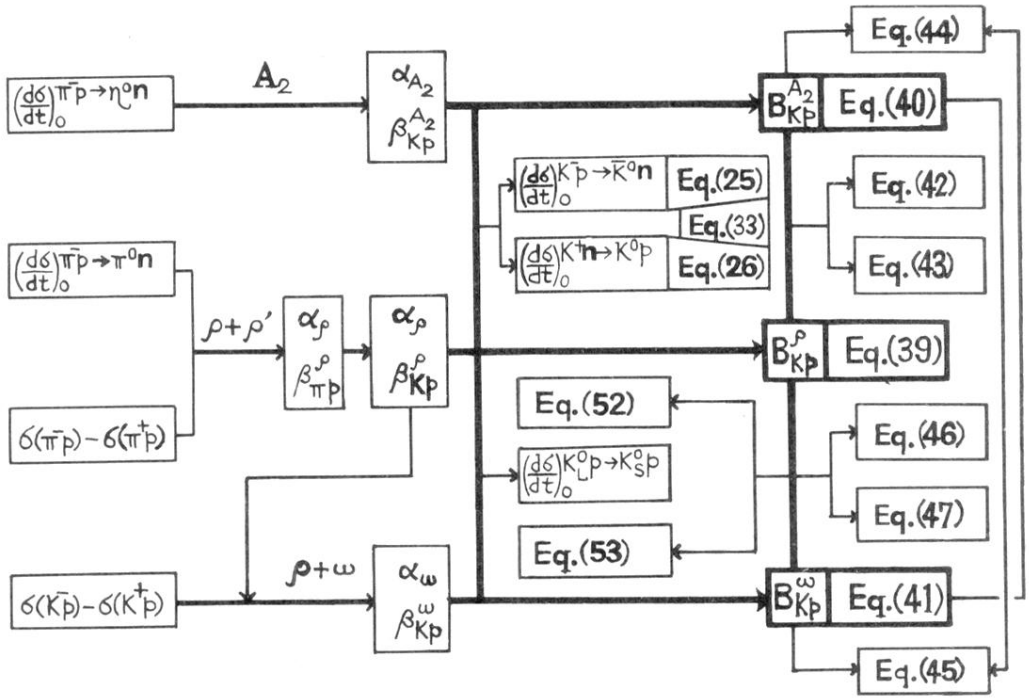

FIG. 1. Schematic diagram for the study of high-energy hadron processes which are mutually combined by Regge parameters. The symbols and equations are explained in the text.

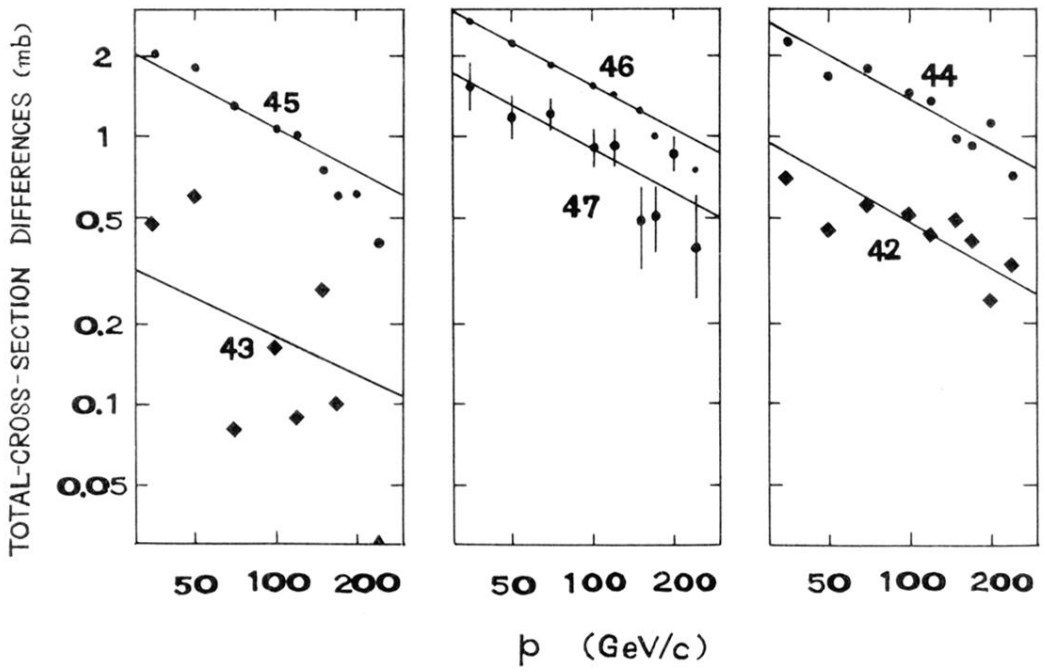

FIG. 2. Comparison of K-N total-cross-section differences between the right-hand side (theoretical prediction: solid line) and the left-hand side (Fermilab data: dot) for Eqs. (42), (43), (44), (45), (46), and (47). Note that the absolute value is shown in the case of Eqs. (43) and (45) since they are always negative. The agreement is excellent, especially at $p = 100$ GeV/c.